Selenomethionine-Substituted *Thermus thermophilus* Cytochrome *ba3*: Characterization of the Cu_A Site by Se and Cu K-EXAFS†

Ninian J. Blackburn,*,‡ Martina Ralle,‡ Ester Gomez,§ Michael G. Hill,§ Andrzej Pastuszyn,|| Donita Sanders,⊥ and James A. Fee*,⊥

Department of Biochemistry and Molecular Biology, Oregon Graduate Institute of Science and Technology, Portland, Oregon 97291-1000, Department of Chemistry, Occidental College, Los Angeles, California 90041, Protein Chemistry Laboratory and Department of Biochemistry, University of New Mexico, Albuquerque, New Mexico 87131-5221, and Department of Biology, University of California at San Diego, La Jolla, California 92093

Received October 20, 1998; Revised Manuscript Received February 22, 1999

ABSTRACT: We have designed a gene that encodes a polypeptide corresponding to amino acids 44−168 of the *Thermus thermophilus* cytochrome ba_3 subunit II [Keightley et al. (1995) *J. Biol. Chem. 270*, 20345−20358]. The resulting ba_3-Cu_{At10} protein separated into two fractions (A and B) during cation exchange chromatography which were demonstrated to differ only by N-terminal acetylation in fraction A. When the gene was expressed in an *Escherichia coli* strain that is auxotrophic for methionine and grown in the presence of selenomethionine (Se(Met)), the single methionine of the Cu_{At10} protein was quantitatively replaced with Se(Met). Native (S(Met)) and Se(Met)-substituted proteins were characterized by electrospray mass, optical absorption, and EPR spectroscopies and by electrochemical analysis; they were found to have substantially identical properties. The Se(Met)-containing protein was further characterized by Se and Cu K-EXAFS which revealed Cu−Se bond lengths of 2.55 Å in the mixed-valence form and 2.52 Å in the fully reduced form of Cu_A. Further analysis of the Se- and Cu-EXAFS spectra yielded the Se−S(thiolate) distances and thereby information on the Se−Cu−Cu and Se−Cu−S(thiolate) angles. An expanded EXAFS structural model is presented.

Cytochrome *c* oxidase serves as the terminal enzyme of the respiratory chain of all eukaryotic cells and of many prokaryotes. It catalyzes the oxidation of cytochrome *c* by dioxygen and simultaneously generates a proton gradient across the membrane by coupling electron transport between internal redox carriers to proton translocation. The primary acceptor of electrons from cytochrome *c* is the Cu_A site located in subunit II, which is the subject of this article. This novel, thiolate-bridged, dinuclear copper center has been extensively characterized by crystallographic, spectroscopic, and electronic structural techniques (*1*−*17*). The chromophore exists in two oxidation states: mixed-valence $Cu^{1.5}$•••$Cu^{1.5}$, designated the oxidized site, and Cu^1•••Cu^1, designated the fully reduced site. Despite the strong electron delocalization and class III character (see above references) of the mixed-valence state, the copper centers are structurally inequivalent. While the bis thiolate core is symmetrical, with each copper coordinated by one terminal histidine residue, the fourth ligand on each copper is different, supplied by methionine-S and a main-chain carbonyl-O, respectively (see Scheme 1).

Because of the relatively low resolution of the present diffraction data, the position of these ligands and their distances to the copper atoms are quite variable in the current crystal structures; hence, their roles in determining the properties of the site are unclear.

Cu K-edge X-ray absorption spectroscopy (XAS)[1] provides high-resolution metrical information on the local environment of metal centers in proteins and has been successfully used to describe coordination of the oxidized and reduced forms of the Cu_A center of *Thermus thermophilus* cytochrome ba_3 (*1*). This work provided convincing evidence that the Cu_2S_2 rhombus exhibits a high degree of structural similarity between oxidized and reduced forms, appearing to require minimal reorganizational energy for electron transfer, thus providing a rationale for the fast electron transfer rates of this site. The remarkably short Cu−Cu distance of 2.43 Å in the oxidized protein increased by 0.07 Å in the reduced form, and small increases in Cu−S distances were also observed on reduction. However, the strong Cu−Cu and

† This research was supported by Grants GM54803 (to N.J.B.) and GM35342 (to J.A.F.) from the National Institutes of Health, by grants from Research Corporation and the Camille and Henry Dreyfus Foundation (to M.G.H.), and by Grant DUE-9551647 from the National Science Foundation (to M.G.H).

* To whom correspondence should be addressed: Ninian J. Blackburn, Department of Biochemistry and Molecular Biology, Oregon Graduate Institute of Science and Technology, P.O. Box 91000, Portland, OR 97291-1000. Tel: 503-748-1384. Fax: 503-748-1464. E-mail: ninian@bmb.ogi.edu. James A. Fee, Department of Biology, University of California at San Diego, La Jolla, CA 92093. Tel: 619-534-4424. Fax: 619-534-0936. E-mail: jfee@ucsd.edu.

‡ Oregon Graduate Institute of Science and Technology.

§ Occidental College.

|| University of New Mexico.

⊥ University of California at San Diego.

[1] Abbreviations: Cu_{At0}, the originally expressed ba_3-Cu_A protein (*18*); Cu_{At10}, corresponds to Cu_{At0} truncated by 10 amino acids; DβM, dopamine β-monooxygenase; DW, Debye−Waller factor; ESMS, electrospray mass spectroscopy; PHM, peptidylglycine α-hydroxylating monooxygense; XAS, X-ray absorption spectroscopy; EXAFS, extended X-ray absorption fine structure.

10.1021/bi982500z CCC: $18.00
Published on Web 05/12/1999

Scheme 1: Schematic View of the Cu_A Site

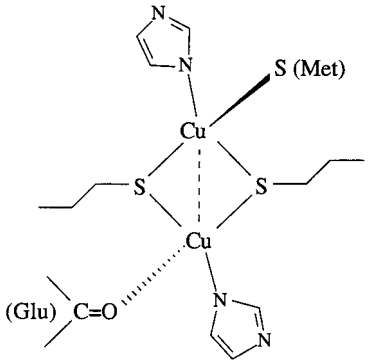

Cu−S interactions which dominated the extended X-ray absorption fine structure (EXAFS) spectrum in the 2.3−2.6 Å region of R-space obscured the weaker interactions from methionine-S and peptide-O coordination. Thus, Cu K-edge XAS failed to identify these weaker ligands.

In this work, we describe a new version of the ba_3-Cu_A protein from *T. thermophilus*, designated ba_3-Cu_{At10}, and procedures for labeling it with selenomethionine (Se(Met)). Since the protein contains a single methionine, which is also the Cu_A ligand, this derivative is expected to have a Se-(Met) residue coordinated to Cu via the Se atom. Optical, EPR, and redox properties of the Se(Met) derivative were compared to those of the S(Met) form and found to be substantially identical. This permitted us to utilize Se K-edge XAS to provide a view of the Cu_A center from the vantage point of the Se atom. This has allowed us to precisely determine the Se−Cu bond length and, by inference, to consider the S(Met)−Cu interaction in the native enzyme. In addition, the weak outer shell interactions present in the Se K-EXAFS have determined the distance of Se to the other atoms of the Cu_2S_2 core, viz the bridging S atoms and the more distant Cu. Merging of the Se K-edge data with complementary metrical information from the Cu K-edge has allowed geometrical positioning of the methionine residue relative to the Cu−Cu axis.

EXPERIMENTAL PROCEDURES

General molecular biology procedures, including several bacterial strains, were as described by Slutter et al. (*18*), except as specified here.

Bacterial Strains. Escherichia coli strain BL21(DE3) from Novagen (Madison, WI) [genotype: F^- *ompT hsdS*$_B$(r_B^- m_B^-) *gal dcm* (DE3)] (*19*) was grown on LB media and was initially used for the expression of the Cu_{At10} fragment. The methionine auxotroph B834(DE3) [genotype F^- *ompT hsdS*$_B$(r_B^- m_B^-) *gal dcm met* (DE3)], obtained from Novagen, was transformed with pETCu_{At10} and used as the expression host in those experiments involving labeled methionine.

Construction of pETCu$_{At10}$. The originally cloned ba_3-Cu_A protein was designed to replace Ile-33 (cf. Figure 8 of ref *20*) with a starting Met residue. [The Cu_A gene was originally cloned into the pET9a (Novagen) vector, but it was subsequently transferred into a compatible multiple cloning site in the Novagen vector pET17b (D. Sanders and J. A. Fee, unpublished data)]. During synthesis of that protein, the N-terminal Met was completely removed by the *E. coli* Met specific aminopeptidase (*21*), leaving a protein with the N-terminal amino acid sequence AYTLATHTAGVIP- - -. This protein is now referred to as ba_3-Cu_{At0} (cf. ref *18*). Here we have designed a protein in which Gly-43 is replaced by Met, and this protein is designated ba_3-Cu_{At10} (indicating a truncation of 10 amino acids). The Cu_A gene in the pET17b plasmid was used to amplify the desired gene product. Oligonucleotides used in the PCR reaction were purchased from Integrated DNA Technologies, Inc. (Coralville, IA). The sense oligonucleotide primer, 5′-d(CACCCACAC-CCAT**ATG**GTCATTC)-3′, was specific for *Thermus* DNA; it contained an *Nde*I site (underlined), the start codon (bold type), and the N-terminal portion of the Cu_{At10} fragment. The antisense oligonucleotide primer, 5′d(TCAAGACCCGTT-TAGAGGCCC)-3′, was complementary to the sequence downstream of the gene for Cu_{At0} and the multiple cloning site in pET17b. DNA amplified from this plasmid using these primers was restricted with *Nde*I and *Bam*HI and ligated into a similarly restricted pET17b plasmid. The protein encoded had the N-terminal sequence MVIPAGK continuing to the C-terminus (cf. Figure 8 of ref *20*). The details of PCR amplification, cloning of the fragment, and verification of its sequence were carried out as described by Slutter et al. (*18*).

Growth of Cells on Se(Met). Despite the toxicity of Se-(Met), it is possible to grow strain B834(DE3) bearing pETCuAt10 on Se(Met). The procedure we used follows closely that described by Budisa et al. (*22*). The cells were initially grown as a small culture (5 mL) in LB media with ampicillin overnight at 37 °C. One milliliter of this was used to inoculate 100 mL of M9 medium supplemented with 2 mM $MgSO_4$, 0.1 mM $CaCl_2$, 0.2% glucose, 0.05% thiamine, and 2 mL of a 50× stock of L-amino acids, minus methionine ("enhanced" M9 medium; cf. ref *23*), and containing 50 μg/mL ampicillin and normal methionine at 20 μg/mL. This culture was incubated overnight at 37 °C. After the cells had begun to recover and grow in this media, 10 mL of this culture was then transferred to 1 L of M9 enhanced minimal media containing 20 μg/mL of Se(Met) plus ampicillin. When the OD_{600} was between 0.4 and 0.8, the culture was brought to 1 mM isopropylthio-β-D-galactoside. The cells were harvested early the following day, but not sooner than 8 h after induction.

Cu_A Protein. Synthesis of the Cu_{At10} protein and its purification were carried out as previously described. The purity ratio $R = A_{790}/A_{280}$ was generally >0.1, being similar to previous preparations of Cu_{At0}. The protein was concentrated to several millimolar and stored frozen at −70 °C to minimize Se oxidation. Protein analyses were done in the Protein Chemistry Laboratory at the University of New Mexico as described by Keightley et al. (*20*). Trypsin digestions were done as follows: In separate tubes, 85 μg of fraction B Cu_{At10} and 93 μg of fraction A Cu_{At10} were dissolved into 100 μL of 0.1 M NH_4HCO_3. Five micrograms of trypsin (Sigma) was added to each tube, incubated at 37 °C for 4 h, and kept frozen until separated on HPLC (*24*). After adjustment of the pH to 2−3, 80 μL aliquots were injected onto a Vydac C18 column (201HS54) equilibrated with 1% solvent B: solvent A, 0.1% trifluoroacetic acid in water; solvent B, 0.1% TFA in 95% acetonitrile, 5% water. Elution of peptides was achieved by a linear gradient of 1% solvent B to 60% solvent B over 60 min. Flow rate was 1 mL/min. Effluent was monitored at 214 nm. Fractions were

collected, frozen, and analyzed by electrospray mass spectroscopy (ESMS) at The Scripps Research Institute Mass Spectrometry facility using a Perkin-Elmer SCIEX API III mass analyzer (Irvine, CA) with the orifice potential set at 100 V (*25*). Holoprotein samples used for ESMS were exchanged into 10 mM ammonium acetate using a small gel filtration column. Reconstructions of mass spectra from ion spectra were made using the SCIEX program BioMulti-View. The GCG (*26*) program PEPTIDESORT was used to calculate expected properties of the isolated gene products.

General Spectral Methods. Optical spectra were recorded on a SLM/AMINCO model DB3500 spectrophotometer in 1 cm cells. The low-temperature EPR spectrum of the native protein was recorded on a Bruker ER-200D spectrometer by Dr. Roland Aasa at Göteborg University while that of the Se(Met)-containing protein was recorded by Mr. Roger Isaacson at the Department of Physics at the University of California−San Diego using a home-built instrument.

Electrochemistry. All electrochemical experiments were performed with a Princeton Applied Research (PAR) model 173 potentiostat driven by a PAR model 175 Universal Programmer. Cyclic voltametry (CV) was performed using a three-electrode configuration consisting of a gold disk working electrode, a platinum auxiliary electrode, and an SCE reference electrode. All three compartments of the electrochemical cell were filled with 0.1 M Tris buffer at pH 8. Gold electrodes were polished with 0.05 μm alumina (Buehler), sonicated for 30 min, and then immersed in a saturated solution of pyridine-4-aldehyde thiosemicarbazone prior to use (*27*).

XAS Data Collection and Analysis. XAS data were collected at the Stanford Synchrotron Radiation Laboratory (SSRL) on beam line 7.3, with a beam energy of 3 GeV and maximum stored beam currents between 100 and 50 mA. The Si(220) monochromator was detuned 50% to reject harmonics. Samples of Cu_{At10} at 2−3 mM in the Cu_A center in 0.05 M Tris-HCl, pH 8, and ~50% in ethyleneglycol were used for EXAFS studies. The fully reduced protein was formed by the addition of a small volume of 1 M sodium ascorbate, and complete reduction was recorded visually before freezing in liquid nitrogen. Samples were shipped on dry ice. Spectra were recorded from frozen aqueous glasses, $T = 10-20$ K, in fluorescence mode using a high-count-rate 13-element Ge detector. To avoid detector saturation, the count rate of each detector channel was kept below 100 kHz. The count rate was controlled by adjusting the hutch entrance slits, or by moving the detector in or out from the cryostat windows. Under these conditions, no dead-time correction was necessary. The summed data for each detector was then inspected, and only those channels that gave high-quality backgrounds free from glitches, drop outs, or scatter peaks were included in the final average. The number of scans included in the averaged spectra were as follows. *T. thermophilus* Se(Met) Cu_A:Se K-edge: oxidized, 10 scans; reduced, 9 scans. Cu K-edge: oxidized, 4 scans; reduced, 4 scans. Se(Met), free amino acid: Se K-edge, 2 scans.

The raw data were averaged, background subtracted, and normalized to the smoothly varying background atomic absorption using the EXAFS data reduction package EXAFSPAK (*28*). The experimental energy threshold ($k = 0$) was chosen as 12 675 eV for the Se K-edge and 8985 eV for the Cu K-edge. Data analysis was carried out by least-squares curve fitting utilizing full curved-wave calculations as formulated by the SRS library program EXCURV98 (*29*−*32*) and methodology described in detail in previous papers (*33*−*35*). The parameters refined in the fit were as follows: E_0, the photoelectron energy threshold; R_i, the distance from Cu to atom i; and $2\sigma^2_i$, the Debye−Waller (DW) term for atom i. Coordination numbers were fixed at the values determined from the crystal structures. The quality of the fits was determined using a least-squares fitting parameter, F, defined as

$$F^2 = (1/N)\sum_i k^6(\chi_i^{\text{theor}} - \chi_i^{\text{exp}})^2$$

referred to as the fit index.

RESULTS

The protein used in these experiments differed from that previously described by Slutter et al. (*18*) by having 10 amino acids removed from the N-terminus. The original purposes in preparing this version of the protein were to facilitate efforts to obtain single crystals that diffracted X-rays to high resolution and to label the protein with Se(Met) in order to utilize the anomalous scattering of the Se atom to obtain phase information. Therefore, the Se(Met) labeling was done with Cu_{At10} rather than Cu_{At0}. With the discovery of conditions that allowed crystallization of the original Cu_{At0} protein and determination of its structure using MAD scattering from the Cu atoms (Williams et al., unpublished data), some initial reasons for working with the truncated version were preempted.[2] This new protein, *ba*$_3$-Cu_{At10}, exhibits some very interesting properties that merit description in the context of this communication.

The properties of the Cu_A center in the Cu_{At10} protein are apparently (see below) identical to those of the *ba*$_3$-Cu_{At0} protein first described by Slutter et al. (*18*). However, Cu_{At10} separates into two fractions during the initial cation chromatography with fraction A preceding fraction B during the development of the CM-Sepharose column (not shown). Both have amino acid compositions expected from the gene sequence (data not shown). Fraction A is N-terminally blocked, whereas fraction B has an N-terminal amino acid sequence showing that the *N*-formyl-Met is removed but is otherwise that expected from the gene fragment VIPAGKL- -. Interestingly, when *E. coli* strain B834(DE3), bearing this gene fragment in our multi-copy plasmid, is grown in the presence of Se(Met), and the Cu_A center is synthesized in the usual manner (*18*), all of the protein chromatographs on CM-Sepharose as if it were in fraction A (not shown). As expected, the N-terminus of the Se(Met)-substituted protein is fully blocked.

Figure 1 shows ESMS of S(Met) containing fractions A and B and the Se(Met) containing *ba*$_3$-Cu_{At0} protein. The predicted mass of the apo-protein from which the *N*-formyl-methionine residue has been removed is 13 818 Da. The mass of the dominant peak in the ESMS of fraction B is 13 942 ± 2 Da which is rationalized as follows: 13 818 + 127(2

[2] Single crystals of *ba*$_3$-Cu_{At10} (fraction B) that diffract to high resolution have been obtained (E. Stura, unpublished data). We have also used this system to prepare *S*-methyl-[$^2H_3$]methionine-substituted protein for magnetic resonance studies (cf. ref *59*).

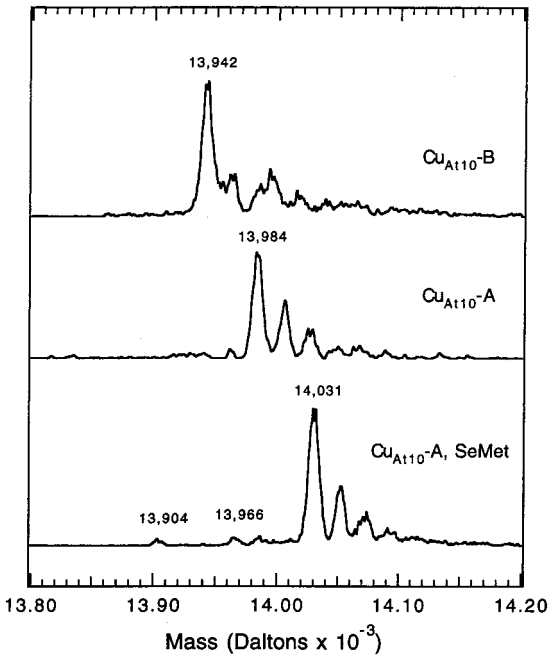

FIGURE 1: Electrospray ionization mass spectra of *T. thermophilus* ba_3-Cu_{At10} proteins. The upper spectrum shows the mass spectrum of the fraction B holoprotein that is separated from the fraction A holoprotein (middle spectrum) during CM-Sepharose chromatography (see ref *18*). While Na^+ ions were largely removed prior to the experiment (see Experimental Section), the ladder of smaller peaks after each primary peak is due to the binding of residual Na^+ (effective mass is 23−1). The lower spectrum is that of the ba_3-Cu_{At10} protein labeled with Se(Met) as described in the Experimental Section. The concentration of proteins was ~2 mg/mL in 10 mM ammonium acetate. The major peaks correspond to the protein having 2 Cu ions bound (see text).

Cu) − 2(2 H from the Cu coordinating thiols) = 13 943 Da, a value within error of the observed molecular mass. The mass of the dominant peak in the ESMS of fraction A is 13 984 ± 2 Da. The difference between the dominant mass of fraction A and that in fraction B is 13 984 ± 2 − 13 942 ± 2 = 42 Da. This corresponds to the mass of CH_3CO, indicating that the N-terminal blocking agent is probably an *N*-acetyl group. *N*-Acetylation of proteins is quite rare in *E. coli*, and little is known about the mechanism (*36*), leading us to seek additional evidence for its occurrence here.

The N-terminus of the Cu_{At10} protein has the following sequence: VIPAGKLERVDPTTVRQEQPW- - - (*20*), and other work has shown that the N-terminus of the Cu_{At0} protein was less structured than the remainder of the protein (ref *18*; Williams, unpublished data). According to PEPTIDESORT, complete digestion of the ba_3-Cu_{At10} apoprotein should lead to two peptides from the N-terminal region having sequences: VIPAGK (583.7 Da, corresponding to the N-terminus of the polypeptide) and VDPTTVR (786.9 Da, corresponding to residues 10−16). If these could be isolated from the two protein fractions and their masses determined, the smaller peptide should be found in both free and N-terminally blocked forms, whereas the larger peptide should have the same mass in both fractions A and B. Therefore, we digested holo-Cu_{At10} (i.e., nondenatured protein) from fractions A and B with trypsin and subjected the resulting digests to HPLC (see Experimental Section). Two low-affinity peaks were observed from both digests, one of which eluted at the same time while the other eluted at different times (data not shown). Each of these fractions was subjected to ESMS. The two peaks obtained from trypsin proteolysis of fraction B (free N-terminus) had masses[3] of 584 and 787 Da, whereas the two peaks obtained from trypsin proteolysis of fraction A (N-terminally blocked) had masses of 627 and 787 Da. Thus, both fractions A and B yield VDPTTVR (787 Da), but only fraction B yields the N-terminal hexapeptide (VIPAGK) predicted by PEPTIDESORT. The fragment having a mass of 584 Da in fraction A is accounted for by adding the mass of the acetyl radical to that of the N-terminal hexapeptide: 584 − 1(H) + 43(acetyl) = 627 Da. These observations indicate that the distinguishing molecular feature of the Cu_{At10} in fraction A is limited to N-terminal acetylation.

The N-terminus of the Se(Met) protein is fully blocked, and we interpret the following ESMS data assuming that the blocking group is *N*-acetyl. The encoded protein contains only one methionine, leading to a predicted mass of the Se(Met)-containing (Se − S = 47 Da), N-terminally acetylated (43 Da) apoprotein of 13 818 + 47 + 43 − 1(H) = 13 907 Da. A small amount of the apoprotein is visible at ~13904 Da (Figure 1). However, the mass of the dominant peak in the ESMS of the Se(Met)-substituted protein is 14 031 ± 2 Da which is rationalized as follows: 13 907 + 127(2 Cu) − 2(2 H) = 14 032 Da, a value within s.e. of the predicted mass. The ESMS results are fully consistent with the known biochemistry of the Cu_{At10} protein and the complete incorporation of one Se atom in place of one S atom when the cells are grown in the presence of Se(Met). We do not understand the origin of the N-terminal acetylation patterns observed for the different Cu_A proteins. However, the presence of the *N*-acetyl group clearly changes the chromatographic properties of the molecule, and because the N-terminus is quite close to the Cu_A center, the properties of the latter might also be affected, although we have no evidence of that.

The visible absorption spectrum of the Se-containing protein is indistinguishable from that of the S(Met)-containing protein (Figure 2). The low-temperature EPR spectra of the Se- and S(Met)-containing proteins are also nominally identical (Figure 3). The g values are $g_z = 2.18_4$ and $g_{xy} = 2.01_9$ for the S protein and $g_z = 2.17_4$ and $g_{xy} = 2.02_5$ for the Se protein. The absence of a significant amount of nonspecifically associated Cu(II) is indicated by the EPR spectrum of the sample used in the EXAFS studies (see below). The electrochemical traces shown in Figure 4 indicate that the redox potentials of the Se(Met)- and the S(Met)-containing proteins are identical at 240 ± 5 mV. The above observations suggest that the Cu_A center in the Se(Met)-containing derivative is essentially identical to that of the native structure[4] and, taken by themselves, might suggest

[3] These peaks are identified by observing a peak in the negative ion region (m − H) that has a corresponding peak at (m + H) in the positive ion region along with an additional peak corresponding to (m + Na).

[4] A similarly complete biochemical and spectroscopic characterization was also carried out on a mutant form of the Cu_{At10} protein in which the Ala residue present at position 84 of ba_3 subunit II had mutated, presumably during PCR amplification, to encode a Thr residue at this position. The methyl carbon of the Ala-84 is buried in the core of the protein and is ~6.3 Å (Williams et al., unpublished data) from the nearest Cu atom. An A84T mutation could thus affect the Cu_A center; however, we found no difference between any of the properties of A84T and native protein. Hence, except where noted, data taken from the two proteins are used interchangeably.

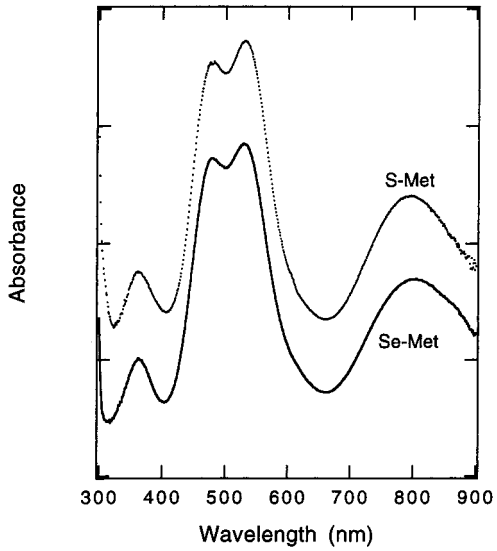

FIGURE 2: Visible optical absorption spectra of the oxidized forms of S(Met) (upper) and Se(Met) (lower) forms of *T. thermophilus* ba_3-Cu_{At10} protein. The spectra were recorded with ~100 μM protein and are offset along the *y*-axis.

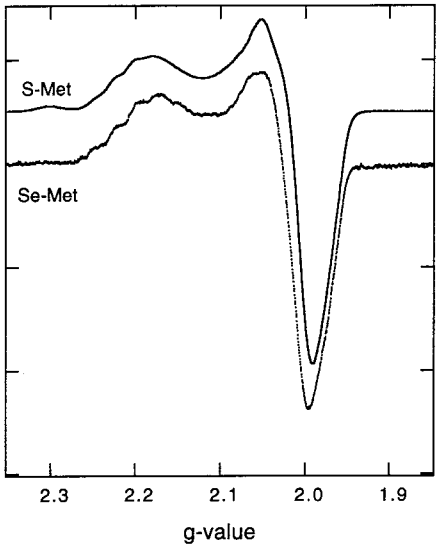

FIGURE 3: Low-temperature X-band EPR spectra of native (S-Met) and selenium-substituted (Se-Met) ba_3-Cu_{At10} protein from *T. thermophilus*. The spectrum of native protein was recorded at 21 K. The microwave frequency was 9.446 GHz, the microwave power was 0.2 milliwatts, the modulation amplitude was 10 G at 100 kHz, the time constant was 100 ms, and the sweep time was 100 s. The spectrum of the Se(Met)-containing protein was recorded at 2.15 K. The microwave frequency was 8.815 GHz, the microwave power was 40 nW, the modulation amplitude was 20 G at 270 Hz, the time constant was 20 ms, and the sweep time was 60 s/1000 G.

that there is at most a very weak interaction between the S(Met) and the Cu_A rhombus. However, the following EXAFS results indicate a significant interaction between the selenium atom of Se(Met) and one of the Cu atoms.

We have measured the Se K-EXAFS of unligated Se(Met) as a ~1 mM aqueous solution and the Se K-EXAFS of the mixed-valence and fully reduced forms of Se(Met)-substituted Cu_A. The resulting data uniquely define the Se−Cu distance and DW factor in both oxidation levels of the protein. The data have also been used in the simulations of the Cu K-EXAFS, resulting in slight adjustments to the XAS structural models previously determined for mixed-valence

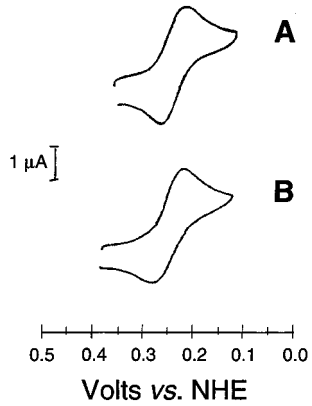

FIGURE 4: Cyclic voltammograms recorded at 25 °C of (A) the Se(Met)-labeled *T. thermophilus* ba_3-Cu_{At10} protein, and (B) isotopically normal ba_3-Cu_{At10} protein. Protein concentrations were ~1 mM, and CVs were recorded at a scan rate of 50 mV/s.

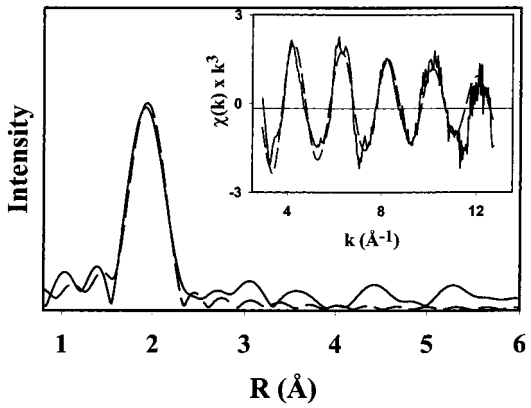

FIGURE 5: Se K-EXAFS of Se(Met)-free amino acid. Experimental (solid line) versus simulated (dashed line) Fourier transform and EXAFS (inset) of a ~1 mM aqueous solution of Se(Met).

and fully reduced *T. thermophilus* Cu_A (*1*).

Selenium Edges. Figure 5 shows Se K-edge XAS [Fourier transform and EXAFS (inset)] for an aqueous solution of uncomplexed Se(Met). The data show a single transform peak corresponding to the two C atoms [Cγ(methylene) and Cδ(methyl)] bonded to Se. Simulation of the data gives a single shell of 2 C at 1.97 Å. Of particular note, the more distant β-C atom of the methionine side chain appears to make a minimal contribution to the EXAFS, as evidenced by the absence of outer-shell peaks in the transform. Thus it is unlikely that contributions from these β-C atoms need be considered in simulations of the EXAFS of Se(Met) coordinated to Cu_A.

Figure 6 shows Se K-EXAFS for oxidized Cu_A. Comparing the Fourier transform with that of the uncomplexed Se(Met) shows an important difference, namely, a prominent second shell peak due to the interaction of Se with the Cu. Simulation of the data yields 2 C at 1.97 Å [Se(Met) Cγ(methylene) and Cδ(methyl)] and 1 Cu at 2.55 Å. The DW term for the C shell is identical to that found in the uncomplexed ligand as expected for the Se−C covalent bonds. However, the DW for the Se−Cu shell is large (0.021 $Å^2$), indicating a weak Cu−Se bond.

Figure 7 shows the corresponding data for the fully reduced protein. A prominent second shell feature is again present, with a significant increase in intensity over that exhibited by the mixed-valence protein. Simulation of these

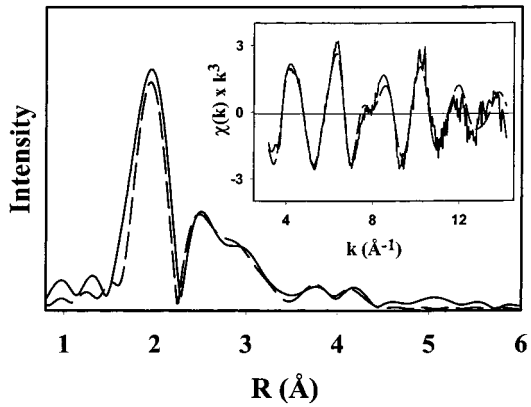

FIGURE 6: Se K-EXAFS of the Se(Met) derivative of oxidized (mixed-valence) *T. thermophilus* Cu_A. Experimental (solid line) versus simulated (dashed line) Fourier transform and EXAFS (inset).

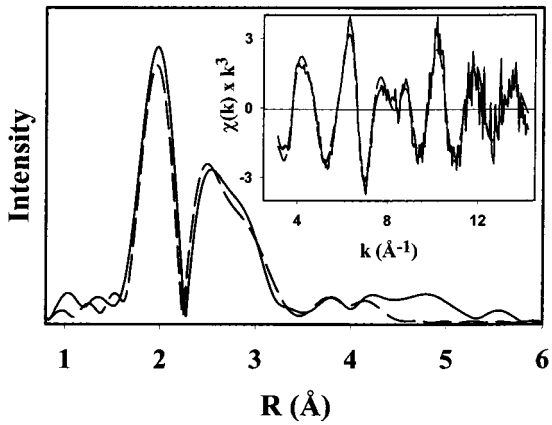

FIGURE 7: Se K-EXAFS of the Se(Met) derivative of fully reduced *T. thermophilus* Cu_A. Experimental (solid line) versus simulated (dashed line) Fourier transform and EXAFS (inset).

data indicates a small increase in the Se−C bond length, 1.99 Å ($\Delta R = 0.02$ Å), and a small decrease in the Se−Cu bond length, 2.52 Å ($\Delta R = 0.03$ Å). The most significant difference is in the magnitude of the DW term for the Se−Cu shell which decreases to 0.015 Å^2 ($\Delta\sigma = 0.005$ Å^2). This suggests that, although the Cu-methionine distance does not change significantly on reduction, the strength of the Cu−Se(Met) bond nevertheless increases.[5]

Close inspection of the outer shell transform peaks of both mixed-valence and fully reduced Se K-edge data sets indicates a well-resolved shoulder on the high *R* side at $R = \sim 3$ Å (phase corrected data). This peak is absent in the uncomplexed Se(Met) data but reproducible between both sets of protein data, suggesting that it arises from a structural element of the Cu_A center. Simulations were attempted utilizing contributions from (i) low Z atoms arising from the imidazole ring of the coordinated histidine, and (ii) S atoms from the bridging thiolate residues. A significant improvement to the fit (16%) was obtained by including a single S scatterer at 3.08 Å in the oxidized fit and 3.06 Å in the reduced fit. Low Z atoms made no improvement to the fit and always refined toward distances of 2.5 Å, which is inconsistent with any plausible structural model. Metrical parameters for the Se K-EXAFS simulations are listed in Table 1.

Copper Edges. The results from the Se EXAFS have defined the distance and DW term for the Cu−Se interaction, enabling these parameters to be fixed in simulations of the Cu EXAFS. This increase in data content has provided a more accurate description of the Cu_A coordination. In previous work, we were unable to detect any contribution from the S atom of the coordinated methionine residue. The 2.55 Å Cu−Se distance determined from the present study and the relatively high DW factor (0.015−0.020 Å^2) provide the explanation, namely, the Cu methionine first shell contribution is overwhelmed by the intense Cu−Cu interaction between 2.4 and 2.5 Å. Simulation of the Cu EXAFS with the Cu−Se(Met) first shell fixed results in small adjustments to the structural parameters of the Cu_2S_2 rhombus previously reported. With the Cu−Se(Met) shell defined, we felt justified in also including the scattering contributions from the glutamate main-chain carbonyl, also excluded from previous fits on the basis of the apparent weak contribution of this shell. For the Se(Met) Cu_A data presented here, the O(Glu) shell (0.5 O/Cu) refines to 2.28 Å in mixed-valence and 2.27 Å in fully reduced with DW terms of 0.003 and 0.004 Å^2, respectively. As with the Cu−Se(Met) interaction, the Cu−O(Glu) contribution overlaps strongly with the Cu−S(cys) shell. However, omitting the O(Glu) from the simulation produced no difference in *F*, and thus the Cu−O(Glu) distance is not well-defined. The alternative conclusion is that the Cu−O(Glu) distance is long and does not contribute to χ(k). The results of these simulations are shown in Figure 8 (oxidized data) and Figure 9 (reduced data) with metrical parameters listed in Table 2.

The structural literature of Cu−Se interactions, while not extensive, indicates a marked preference for selenides and Se-containing ligands to form complexes with the Cu(I) oxidation state (*37*−*42*). For example, Cu(II) complexes of selenoethers are known to undergo spontaneous reduction and demetalation to yield species containing Se−Se bonds (*43*). The coordination chemistry of copper selenolates and selenoethers is predominately polynuclear, with both terminal and bridging Se atoms present in the structures. For selenides and selenolates, Cu−Se distances range from 2.30 to 2.44 Å (*37*−*42*), while for selenoethers there is a tendency toward longer distances (2.42−2.52 Å) (*43*−*45*). Se(Met) derivatives of cupredoxins have been reported to have resonance Raman spectra identical to those of the naturally occurring S(Met) proteins (*46*), but no EXAFS data on the Cu−Se bond lengths were reported. The Cu−Se distance for Se(Met) Cu_A thus appears to be just on the high side of the normal range for Cu(I)−Se selenoether bonds. Se−C bonds for Cu selenoethers are close to 1.96 Å for aliphatic C atoms (methyl, methylene) bonded to Se and compare well with the Cu−C distance of 1.97 Å determined by EXAFS for the Se(Met) Cu_A site.

Considerations of outer shell interactions in the Se K-EXAFS from more distant scattering atoms of the Cu_2S_2 rhombus have been combined to further refine the EXAFS-derived view of the *T. thermophilus* Cu_A center. The pronounced shoulder on the high *R* side of the second shell of the Fourier transform can be fit well to a single S atom at

[5] Se K-edge data (not shown) on the A84T mutant protein gave reproducible Se−Cu distances for oxidized and reduced forms within experimental error (R/Å, ($2\sigma^2$/Å^2) = 2.54 (0.030), oxidized; 2.49 (0.015), reduced). However, the difference in Debye−Waller factors ($\Delta\sigma = 0.015$ Å^2) between oxidized and reduced forms was even more pronounced.

Table 1: Parameters Used To Simulate the Se K-Edge of Se(Met) Derivatives of the Cu_A Center of *Thermus thermophilus* Cytochrome ba_3[a]

		Se−C (2)		Se−Cu1 (1)		Se−S1 (1)		Se−Cu2 (1)		Se−S2 (1)	
	F	R (Å)	$2\sigma^2$ (Å^2)	R (Å)	$2\sigma^2$ (Å^2)	R (Å)	$2\sigma^2$ (Å^2)	R (Å)	$2\sigma^2$ (Å^2)	R (Å)	$2\sigma^2$ (Å^2)
oxidized	0.67	1.97	0.005	2.55	0.020	3.08	0.025	3.79	0.022	4.10	0.013
reduced	0.70	1.99	0.004	2.52	0.015	3.06	0.018	3.82	0.022	4.12	0.012
free amino acid	1.06	1.97	0.006								

[a] Coordination numbers for each scatterer are given in parentheses. Distances are estimated to be accurate ±0.01 Å for R < 3 Å and ±0.03 Å for R > 3 Å.

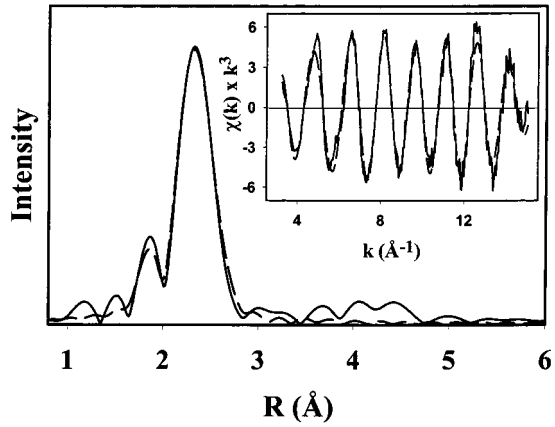

FIGURE 8: Cu K-EXAFS of the Se(Met) derivative of oxidized (mixed-valence) *T. thermophilus* Cu_A. Experimental (solid line) versus simulated (dashed line) Fourier transform and EXAFS (inset).

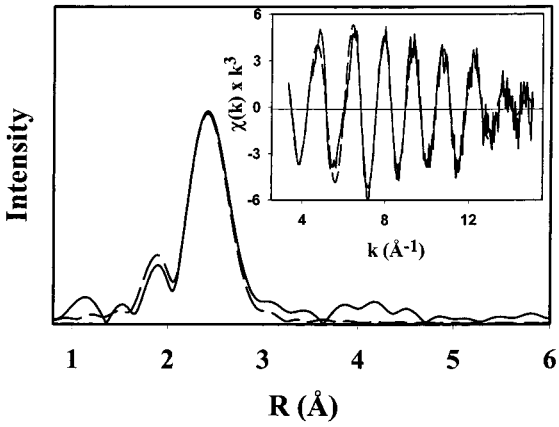

FIGURE 9: Cu K-EXAFS of the Se(Met) derivative of fully reduced *T. thermophilus* Cu_A. Experimental (solid line) versus simulated (dashed line) Fourier transform and EXAFS (inset).

Table 2: Parameters Used To Simulate the Cu K-Edge of Se(Met) Derivatives of the Cu_A Center of *Thermus thermophilus* Cytochrome ba_3[a]

		Cu−N(His)		Cu−S(Cys)		Cu−Cu		Cu−Se(Met)	
	F	R (Å)	$2\sigma^2$ (Å^2)	R (Å)	$2\sigma^2$ (Å^2)	R (Å)	$2\sigma^2$ (Å^2)	R (Å)	$2\sigma^2$ (Å^2)
oxidized	0.33	1.94	0.002	2.25	0.009	2.43	0.004	2.55	0.020
reduced	0.45	1.96	0.002	2.28	0.013	2.50	0.006	2.52	0.015

[a] Coordination numbers in the simulations were fixed at 1.0 N, 2.0 S, 1.0 Cu, and 0.5 Se scatterers per Cu_A absorber. Distances are estimated to be accurate to ±0.01 Å.

3.09 Å. The only plausible candidate for this interaction is one of the bridging thiolates, and the following question arises: Where is the contribution from the second thiolate S? Close inspection of the transform data for the mixed-valence protein reveals two additional weak peaks around 4 Å which can be fit to a S at 4.10 Å (the second thiolate) and the more distant Cu scatterer at 3.79 Å. Because of the low intensity of these peaks, their interpretation should be treated with caution. Nevertheless, the peaks are reproducible in both the oxidized and reduced Se K-edge data and in the data from the A84T mutant protein.[4,5] The metrical parameters for these outer shell interactions are given in Table 1.

As shown in Figure 10, knowledge of Se−S1(thiolate), Se−S2(thiolate), Se−Cu1, and Se−Cu2 distances from the Se K-EXAFS can be combined with Cu−S(thiolate) and Cu−Cu distances from the Cu-K-EXAFS to precisely determine the position of the Se atom. As shown in the figure, these distances define the sides of three triangles with Se at a common apex. If the Cu_2S_2 plane is fixed in space, only two of these triangles are necessary to precisely define the coordinates of the Se atom (actually two symmetry-related positions above and below the plane) The third triangle can be used to provide an independent check on the validity of the EXAFS-derived distances. With the use of molecular modeling, it has been possible to position the Se atom such that all of the EXAFS-derived bond lengths in the triangles Se−Cu−S1 and Se−Cu−S2 are satisfied. Using the Se−Cu1−Cu2 triangle (Cu1−Cu2 = 2.42 Å), a Se−Cu2 distance of 3.81 Å can be calculated, in excellent agreement with the experimentally determined value of 3.79 Å.

DISCUSSION

The Se(Met)-substituted ba_3-Cu_{At10} protein is a well-defined molecule in which a single Se atom has replaced the S(Met) atom as a first-shell ligand to the Cu_A center. The essential identity of the optical and EPR spectra of the mixed-valence form and the identity of the redox potentials suggest that whatever role the S(Met) atom plays in cluster stability and electronic properties is also carried out by the Se(Met) atom. While the simplest interpretation might be that there is no significant interaction of the Se/S(Met) atom with the Cu_A rhombus, the Se K-edge XAS results provide unequivocal evidence for an Se−Cu bond.

Accordingly, the present data provide the first structural information on the possible role of methionine at the Cu_A center. There are two important conclusions: The Cu−Se(Met) bond length is insensitive to the Cu_A redox state and appears to be longer than expected in comparison to low-molecular-weight Cu(I) selenoethers. Thus, the Cu_A cluster is essentially isostructural in the mixed-valence and fully reduced forms, from which it is surmised that the reorganization energy should be correspondingly small (*47*). Further, if the Cu−Se/S(Met) bond length is in fact extended beyond a normal value, then questions arise as to whether the protein matrix imposes this isostructural condition, as might be predicted from "entatic state" ideas (see below), or whether the bonding within the Cu_A rhombus is sufficiently strong

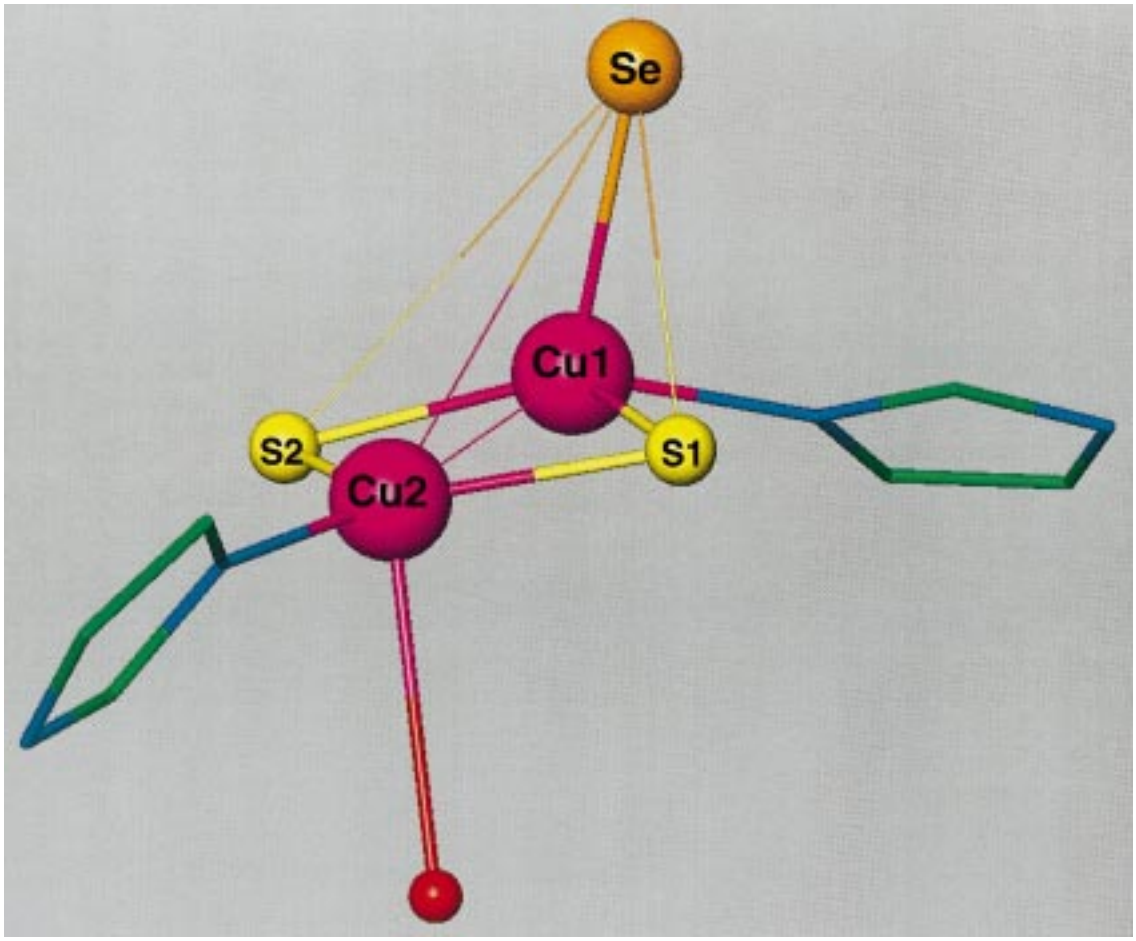

FIGURE 10: Positioning of the Se atom of the Se(Met) derivative of the oxidized *T. thermophilus* Cu_A via merging of the metrical data obtained from both the Se and Cu edges. For details, see the text.

to be largely insensitive to the geometry and nature of the nonimidazole exoligands.

Methionine coordination occurs in two other classes of copper proteins. Cupredoxins have three strongly bonded ligands in an approximately trigonal planar arrangement, with a very weakly coordinated methionine at 2.6−3.0 Å. In some cases, there is a fifth weak interaction with a peptide carbonyl oxygen in an axial position roughly trans to the methionine. Like Cu_A, redox cycling between the Cu(II) and Cu(I) forms produces only small changes in the geometry of the site, including the position of the methionine ligand. Also like Cu_A, the spectral features of the blue copper site are insensitive to substitution with Se(Met) (*46*). The coordination of the copper center appears to be poised midway between the preferred coordination environments for Cu(II) and Cu(I) which has led to the now generally accepted idea (the "entatic state" hypothesis) that the protein matrix imposes a strained environment on the metal center in which the energy of protein deformation exceeds that of reorganization of metal site geometry (*48*−*51*). In this way, the reorganizational energy for electron transfer is kept to a minimum. Indeed, electronic structural calculations and consideration of optimal distances for Cu(II)− and Cu(I)−S(thioether) bonds suggest the conclusion that the entatic nature of the blue copper site involves restriction of the movement of the methionine ligand in both oxidized and reduced states (*47*, *52*).

The Cu−S(Met) coordination found in peptidylglycine monooxygenase (PHM) and dopamine-β-monooxygenase (DβM) contrasts dramatically with that found in cupredoxins. These proteins contain two structurally distinct mononuclear copper centers. The polypeptide provides three histidines as ligands for the A-copper site and two histidines and a methionine as ligands for the B-copper site (*53*−*55*). X-ray crystallography of PHM (*54*), and XAS of PHM (*53*, *55*) and DβM (*34*) indicate that both copper centers are highly solvent-accessible. Neither of these proteins possesses unusual EPR or optical absorption properties indicative of an entatic contribution to the individual Cu sites. In fact, the reverse effect seems to operate, since EXAFS spectroscopy has identified a large catalytically significant structural change on reduction, involving the movement of the methionine-S atom at the B−Cu from a distance in excess of 2.6 Å in the oxidized protein to 2.25 Å in the reduced protein. Thus, in a protein where spectral signs suggest the absence of entatic state effects, the interaction of the Cu(II) center with the methionine-S atom is weak, and strong Cu−S bonding is only achieved in the Cu(I) valence state. These observations would seem to confirm that the true origin of the entatic state in cupredoxins is the ability to prevent the movement of the S(Met) atom close to the Cu(I) center in the reduced forms of the blue copper sites, thereby avoiding an overly strong stabilization of the Cu(I) form.

Supporting evidence for this proposal comes from the H117G and H46G mutants of azurin where reduction is irreversible. It has been suggested that these mutations can relax the entatic state leading to a stable 3-coordinate Cu(I) complex with one histidine, one cysteine, and one methionine

as ligands (*56*), the soft methionine ligand presumably moving closer to the Cu(I). A similar effect appears to occur when azurin is unfolded (*57*) which leads to an increase of 130 mV in midpoint potential, perhaps as the result of a stronger interaction between Cu(I) and the soft methionine ligand. However, X-ray structural data on an M121H mutant of azurin has challenged the concept of the entatic state in this protein, since (i) at neutral pH the H121 imidazole Nδ has moved to within 2.24 Å of the Cu(II) center, and (ii) a low pH form of this mutant exhibits a strongly perturbed protein conformation in the vicinity of the Cu(II) as the result of movement of the protonated H121 out of the copper coordination sphere (*58*). Clearly, the repulsion introduced by attempting to position a protonated imidazole close to the positively charged Cu(II) center can overcome the energy required for local refolding of the polypeptide.

The Cu−Se distance in the *ba*$_3$-Cu_{At10} protein of 2.54 Å in both mixed-valence and fully reduced protein is suggestive of an entatic state. If we assume that Cu−S and Cu−Se bond lengths are comparable (*37*), we estimate that the Cu−S(Met) distance is approximately 0.3 Å longer than expected for an unrestrained Cu−S(thioether) bond, based on the EXAFS-determined Cu−S(thioether) interaction in PHM, Cu−S = 2.25 Å, DW = 0.006 (see above). The DW term for the mixed-valence Cu−Se interaction is in the range 0.02−0.03 Å^2, indicative of a weak Cu−Se bond. However, despite the negligible change in Cu−Se distance, the DW term for the Cu−Se interaction in the reduced protein is between 25% and 50% smaller,[5] indicative of a substantial increase in bond strength. This argues in favor of a protein-induced interplay between the opposing forces, tending to optimize Cu(I)-Se-(S) bonding interactions and those tending to preserve the protein fold and hence the metal site geometry. If, on the other hand, Cu(I)−S(ether) bonds are 0.16−0.18 Å shorter than Cu(I)−Se(ether) bonds as stated by Batchelor et al. (*43*), then the expected length of the Cu−S(Met) bond in native Cu_A is ∼2.47 Å. This would suggest substantial interaction of the S(Met) with the CuA center and, if true, would indicate that the bonding within the Cu_A rhombus is quite insensitive to the nature of the nonimidazole exoligands. In this case, it should be possible to prepare Cu_A centers with a variety of exoligands.[6]

ACKNOWLEDGMENT

We thank Roland Aasa and Roger Isaacson for recording the EPR spectra, and we thank Gary Siuzdak for providing access to the mass spectroscopy facility at The Scripps Research Institute as well as helpful discussions on the interpretation of the spectra. We gratefully acknowledge the use of facilities at the Stanford Synchrotron Radiation Laboratory (SSRL), which is supported by the National Institutes of Health Biomedical Research Technology Program, Division of Research Resources, and by the Department of Energy, Office of Health and Environmental Research.

[6] The exoligands could play an essential role in guiding Cu_A synthesis without having much effect on Cu_A stabilization. Thus, simple failure to form the Cu_A center in a particular mutant protein may not be very informative.

NOTE ADDED IN PROOF

The crystal structure of the *ba*$_3$-Cu_{At0} protein has recently been determined to 1.6 Å resolution [Williams, P. A., Blackburn, N. J., Sanders, D., Bellamy, H., Stura, E. A., Fee, J. A., and McCree, D. E. (1999) *Nat. Struct. Biol.* (in press).].

REFERENCES

1. Blackburn, N. J., de Vries, S., Barr, M. E., Houser, R. P., Tolman, W. B., Sanders, D., and Fee, J. A. (1997) *J. Am. Chem. Soc. 119*, 6135−6143.
2. Williams, K. R., Gamelin, D. R., Lacroix, L. B., Houser, R. P., Tolman, W. B., Mulder, M. C., de Vries, S., Hedman, B., Hodgson, K. O., and Solomon, E. I. (1997) *J. Am. Chem. Soc. 119*, 613−614.
3. Andrew, C. R., and Sanders-Loehr, J. (1996) *Acc. Chem. Res. 29*, 365−372.
4. Andrew, C. R., Fraczkiewicz, R., Czernuszewicz, R. S., Lappaleinen, P., Saraste, M., and Sanders-Loehr, J. (1996) *J. Am. Chem. Soc. 118*, 10436−10445.
5. Farrar, J. A., Neese, F., Lappalainen, P., Kroneck, P. M. H., Saraste, M., Zumft, W. G., and Thompson, A. J. (1996) *J. Am. Chem. Soc. 118*, 11501−11514.
6. Karpefors, M., Slutter, C. E., Fee, J. A., Aasa, R., Kallebring, B., Larsson, S., and Vanngard, T. (1996) *Biophys. J. 71*, 2823−2829.
7. Neese, F., Zumft, W. G., Antholine, W. G., and Kroneck, P. M. H. (1996) *J. Am. Chem. Soc. 118*, 8692−8699.
8. Andrew, C. R., Lappalainen, P., Saraste, M., Hay, M. T., Lu, Y., Dennison, C., Canters, G. W., Fee, J. A., Slutter, C. E., Nakamura, N., and Sanders-Loehr, J. (1995) *J. Am. Chem. Soc. 117*, 10759−10760.
9. Farrar, J. A., Lappalainen, P., Zumft, W. G., Saraste, M., and Thompson, A. J. (1995) *Eur. J. Biochem. 232*, 294−303.
10. Iwata, S., Ostermeier, C., Ludwig, B., and Michel, H. (1995) *Nature 376*, 660−669.
11. Tsukihara, T., Aoyama, H., Yamashita, E., Tomizaki, T., Yamaguchi, H., Shinzawa-Itoh, K., Nakashima, R., Yaono, R., and Yoshikawa, S. (1995) *Science 269*, 1069−1074.
12. Wilmanns, M., Lapplalainen, P., Kelly, M., Sauer-Eriksson, E., and Saraste, M. (1995) *Proc. Natl. Acad. Sci. U.S.A. 92*, 11955−11959.
13. Andrew, C. R., Han, J., de Vries, S., van der Oost, J., Averill, B. A., Loehr, T. M., and Sanders Loehr, J. (1994) *J. Am. Chem. Soc. 116*, 10805−10806.
14. von Wachenfeldt, C., de Vries, S., and van der Oost, J. (1994) *FEBS Lett. 340*, 109−113.
15. Kelly, M., Lappalainen, P., Talbo, G., Haltia, T., van der Oost, J., and Saraste, M. (1993) *J. Biol. Chem. 268*, 16781−16787.
16. Lappalainen, P., Aasa, R., Malmstrom, B. G., and Saraste, M. (1993) *J. Biol. Chem. 268*, 26416−26421.
17. van der Oost, J., Lappalainen, P., Musacchio, A., Warne, A., Lemieux, L., Rumbley, J., Gennis, R. B., Aasa, R., Pascher, T., Malmstrom, B. G., and Saraste, M. (1992) *EMBO J. 11*, 3209−3217.
18. Slutter, C. E., Sanders, D., Wittung, P., Malmström, B., Aasa, R., Richards, J. H., Gray, H. B., and Fee, J. A. (1996) *Biochemistry 35*, 3387−3395.
19. Studier, F. W., and Moffatt, B. A. (1986) *J. Mol. Biol. 189*, 113−130.
20. Keightley, J. A., Zimmermnn, B. H., Mather, M. W., Springer, P., Pastuszyn, A., Lawrence, D. M., and Fee, J. A. (1995) *J. Biol. Chem. 270*, 20345−20358.
21. Miller, C. G. (1987) in *Escherichia coli and Salmonella typhimurium* (Neidhardt, F. C., Ed.) pp 680−691, ASM Press, New York.
22. Budisa, N., Steipe, B., Demange, P., Eckerskorn, C., Kellermnn, J., and Huber, R. (1995) *Eur. J. Biochem. 230*, 788−796.
23. Cutting, S. M., and Youngman, P. (1994) in *Methods for General and Molecular Biology* (Murray, R. G. E., Wood, W. A., and Krieg, N. R., Eds.) pp 348−364, ASM Press, Washington, DC.

24. Aitken, A., Geisow, M. J., Findlay, J. B. C., Holmes, C., and Yarwood, A. (1989) in *Protein Sequencing, a Practical Approach* (Findlay, J. B. C., and Geisow, M. J., Eds.) p 58, IRL Press, Oxford, U.K.
25. Siuzdak, G. (1994) *Proc. Natl. Acad. Sci. U.S.A. 91*, 11290−11297.
26. Devereux, J., Haeberli, P., and Smithies, O. (1984) *Nucleic Acids Res. 12*, 387−395.
27. Immoos, C., Hill, M. G., Sanders, D., Fee, J. A., Slutter, C. E., Richards, J. H., and Gry, H. B. (1996) *J. Biol. Inorg. Chem. 1*, 529−531.
28. George, G. N. (1990) Stanford Synchrotron Radiation Laboratory.
29. Gurman, S. J. (1989) in *Synchrotron Radiation and Biophysics* (Hasnain, S. S., Ed.) pp 9−42, Ellis Horwood Ltd., Chichester, U.K.
30. Binsted, N., Gurman, S. J., and Campbell, J. W. (1988) *Daresbury Laboratory EXCURV88 Program*.
31. Gurman, S. J., Binsted, N., and Ross, I. (1986) *J. Phys. C: Solid State Phys. 19*, 1845−1861.
32. Gurman, S. J., Binsted, N., and Ross, I. (1984) *J. Phys. C: Solid State Phys. 17*, 143−151.
33. Sanyal, I., Karlin, K. D., Strange, R. W., and Blackburn, N. J. (1993) *J. Am. Chem. Soc. 115*, 11259−11270.
34. Blackburn, N. J., Hasnain, S. S., Pettingill, T. M., and Strange, R. W. (1991) *J. Biol. Chem. 266*, 23120−23127.
35. Strange, R. W., Blackburn, N. J., Knowles, P. F., and Hasnain, S. S. (1987) *J. Am. Chem. Soc. 109*, 7157−7162.
36. Persson, B., Flinta, C., von Heijne, G., and Jörnvall, H. (1985) *Eur. J. Biochem. 152*, 523−527.
37. Hong, M., Zhang, Q., Cao, R., Wu, D., Chen, J., Zhang, W., Liu, H., and Lu, J. (1997) *Inorg. Chem. 36*, 6251−6260.
38. Cheng, Y., Emge, T. J., and Brennan, J. G. (1996) *Inorg. Chem. 35*, 7339−7344.
39. Raymond, C. C., and Dorhout, P. K. (1996) *Inorg. Chem. 35*, 5634−5641.
40. Yam, V. W.-W., Lo, K. K.-W., and Cheung, K.-K. (1996) *Inorg. Chem. 35*, 3459−3462.
41. Salm, R. J., and Ibers, J. A. (1994) *Inorg. Chem. 33*, 4216−4220.
42. Christuk, C. C., Ansari, M. A., and Ibers, J. A. (1992) *Inorg. Chem. 31*, 4365−4369.
43. Batchelor, R. J., Einstein, F. W. B., Gay, I. D., Gu, J.-H., Pinto, M., and Zhou, X.-M. (1990) *J. Am. Chem. Soc. 112*, 3706−3707.
44. Black, J. R., Champness, N. R., Levason, W., and Reid, G. (1996) *Inorg. Chem. 35*, 1820−1824.
45. Batchelor, R. J., Einstein, F. W. B., Gay, I. D., Gu, J.-H., and Pinto, B. M. (1991) *J. Organomet. Chem. 411*, 147−157.
46. Thamann, T. J., Frank, P., Willis, L. J., and Loehr, T. M. (1982) *Proc. Natl. Acad. Sci. U.S.A. 79*, 6396−6400.
47. Ramirez, B. E., Malmstrom, B. G., Winkler, J. R., and Gray, H. B. (1995) *Proc. Natl. Acad. Sci. U.S.A. 92*, 11949−11951.
48. Holm, R. H., Kennepohl, P., and Solomon, E. I. (1996) *Chem. Rev. 96*, 2239−2314.
49. Vallee, B. L., and Williams, R. J. P. (1968) *Proc. Natl. Acad. Sci. U.S.A. 59*, 498−505.
50. Lindskog, S., and Malmstrom, B. G. (1962) *J. Biol. Chem. 237*, 1129−1138.
51. Malmstrom, B. G., and Vanngard, T. (1960) *J. Mol. Biol. 2*, 118−124.
52. Solomon, E. I., Baldwin, M. J., and Lowery, M. L. (1992) *Chem. Rev. 92*, 521−542.
53. Ralle, M., Jaron, S., Rhames, F., Eipper, B. A., Mains, R. E., and Blackburn, N. J. (1998) *Biochemistry* (submitted for publication).
54. Prigge, S. T., Kolhekar, A. S., Eipper, B. A., Mains, R. E., and Amzel, L. M. (1997) *Science 278*, 1300−1305.
55. Boswell, J. S., Reedy, B. J., Kulathila, R., Merkler, D. J., and Blackburn, N. J. (1996) *Biochemistry 35*, 12241−12250.
56. van Pouderoyen, G., Andrew, C. R., Loehr, T. M., Sanders-Loehr, J., Mazumdar, S., Hill, H. A. O., and Canters, G. W. (1996) *Biochemistry 35*, 1397−1407.
57. Leckner, J., Wittung, P., Bonander, N., Karlsson, B. G., and Malmstrom, B. G. (1997) *J. Biol. Inorg. Chem. 2*, 368−371.
58. Messerschmidt, A., Prade, L., Kroes, S. J., Sanders-Loehr, J., Huber, R., and Canters, G. W. (1998) *Proc. Natl. Acad. U.S.A. 95*, 3443−3448.
59. Bertini, I., Bren, K., Clemente, A., Fee, J. A., Gray, H. B., Luchinat, C., Malmström, Richards, J. H., Sanders, D., and Slutter, C. E. (1996) *J. Am. Chem. Soc. 118*, 11658−11659.

BI982500Z